

Contents

1.	Experimental Section	2
2.	Mass spectra of monolayers S1, S3-S6, S10, S11, S _{mix}	3
a)	Mass spectrum of S1	3
b)	Mass spectrum of S3	5
c)	Mass spectrum of S4	6
d)	Mass spectrum of S5	7
e)	Mass spectrum of S6	8
f)	Mass spectrum of S10	9
g)	Mass spectrum of S11	10
h)	Mass spectrum of S _{mix}	11
3.	XPS analysis of monolayers S1-S6, S10, S11, S _{mix}	12
4.	Detected ions on monolayers S1-S11 and S _{mix}	14
5.	Limit of detection of DART-HRMS	15
6.	References	15
7.	Acknowledgements.....	15

1. Experimental Section

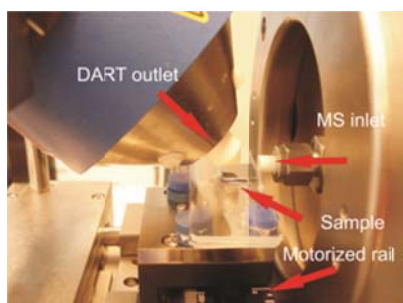


Figure S1. Experimental set-up of DART-HRMS: DART outlet (at 45°); ceramic tube which guides the ions to the MS inlet; sample, immobilized on a glass slide; motorized rail moving the sample between DART outlet and MS inlet.

All chemicals and solvents were purchased from Sigma-Aldrich and used as received unless stated otherwise. The cyclooctyne derivative (**11**) was purchased from SynAffix, B.V., The Netherlands. The synthesis of **1** and surface chemistry reactions on Si_3N_4 were described elsewhere.^[1]

All modified Si_3N_4 specimens were sized between 0.7 cm and 1.5 cm. The modified samples were immobilized together with a reference sample on a glass slide, using double-sided tape. The minimum distance between the specimens was at least 1 cm. Before analysis all samples were cleaned by exhaustive sonication in appropriate solvents for at least 15 min and afterwards dried under argon. Before analysis with DART-HRMS all samples were analyzed with XPS to confirm the successful formation of the monolayers. The XPS spectra of each monolayer are shown in Fig. S11 and S12. After XPS analysis, they were stored till analysis with DART-HRMS in a glove box (MBraun MB200G & MBraun MB20G) under an argon atmosphere with a content of H_2O and O_2 each below 0.1 ppm. The DART-orbitrap MS system consisted of a DART ion source (model DART-SVP, IonSense, Saugus, USA) coupled to an Exactive high-resolution mass spectrometer (Thermo Fisher Scientific, San Jose, CA, USA). The mass spectrometer was calibrated at the beginning of each day. XCALIBUR software (v. 2.1) was used for instrument control, data acquisition and data processing. The distance between mass inlet and the DART outlet was kept at ~1 cm. The samples were placed between them in such a way that one side of the specimen was as close as possible to ceramic transfer tube of the DART-MS interface. The DART outlet was pointed at an angle 45° to the surface and the height was adjusted to be as close as possible to the surface while still avoiding direct contact and, thus contamination of the outlet. The temperature was kept at 450 °C during all surface analyses.

DART settings in (+)-mode were: He as ionizing gas, fixed flow of ~3.5 L/min; gas beam temperature set at 450 °C; grid electrode voltage +350 V. MS: capillary voltage +80 V; tube lens voltage +185 V; skimmer voltage +42 V; capillary temperature: 275 °C. The resolution was set at “ultra high” and a scan rate of 1 Hz was used. The mass range was m/z 50–500.

DART settings in (-)-mode were: He as ionizing gas, fixed flow of ~3.5 L/min; gas beam temperature set at 450 °C; grid electrode voltage -350 V. MS: capillary voltage -50 V; tube lens voltage -100 V; skimmer voltage -20 V; capillary temperature: 275 °C. The resolution was set at “ultra high” and a scan rate of 1 Hz was used. The mass range was m/z 50–300.

DART settings in (+)-mode were additionally optimized for the simultaneous analysis of all six ions in monolayer \mathbf{S}_{mix} : He as ionizing gas, fixed flow of ~3.5 L/min; gas beam temperature set at 450 °C; grid electrode voltage +350 V. MS: capillary voltage +25 V; tube lens voltage +50 V; skimmer voltage +18 V; capillary temperature: 275 °C. The resolution was set at “ultra high” and a scan rate of 1 Hz was used. The mass range was m/z 100–300.

Only ions with a mass accuracy of 1 mmu or less were accepted. In few cases, a mass shift higher than 1 mmu was observed. This was due to their low relative abundance and the presence of adjacent intense isobaric peaks. Under these conditions, a mass shift can occur due to phenomena described elsewhere.^[2]

2. Mass spectra of monolayers **S1**, **S3-S6**, **S10**, **S11**, **S_{mix}**

a) Mass spectrum of **S1**

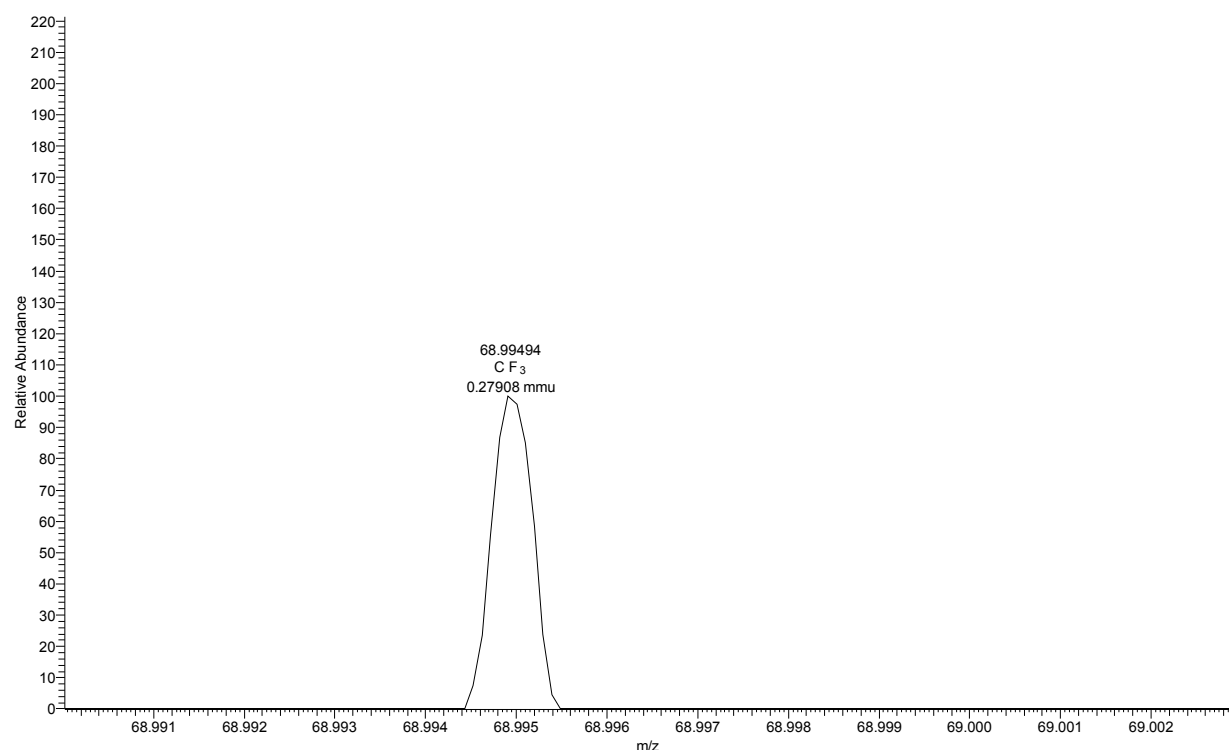


Figure S2. Negative mode DART-Orbitrap mass spectrum from m/z 68.990-69.003 of **S1**. Peak at m/z 68.99494 is $[\text{CF}_3]^-$.

meting010_TFE #281 RT: 4.13 AV: 1 NL: 5.63E2
T: FTMS - p NSI Full ms [50.00-300.00]

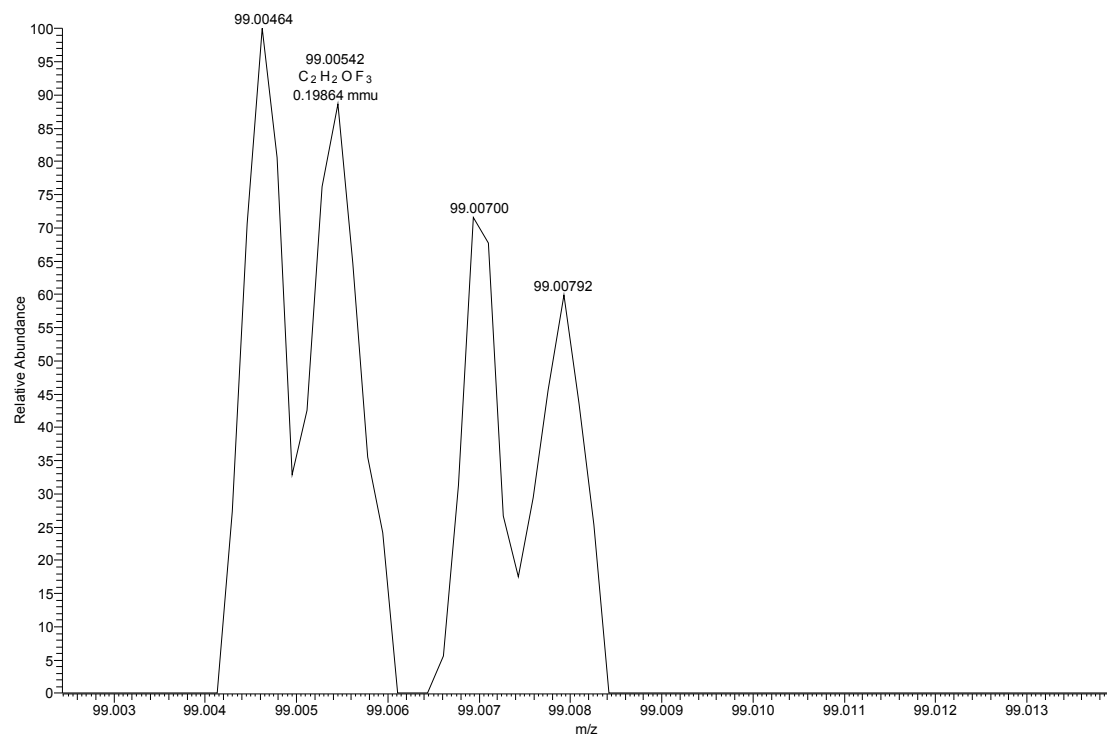


Figure S3. Negative mode DART-Orbitrap mass spectrum from m/z 99.002-99.014 of **S1**. Peak at m/z 99.00542 is $[\text{M}-\text{H}]^-$, where M is $\text{CF}_3\text{CH}_2\text{OH}$.

b) Mass spectrum of **S3**

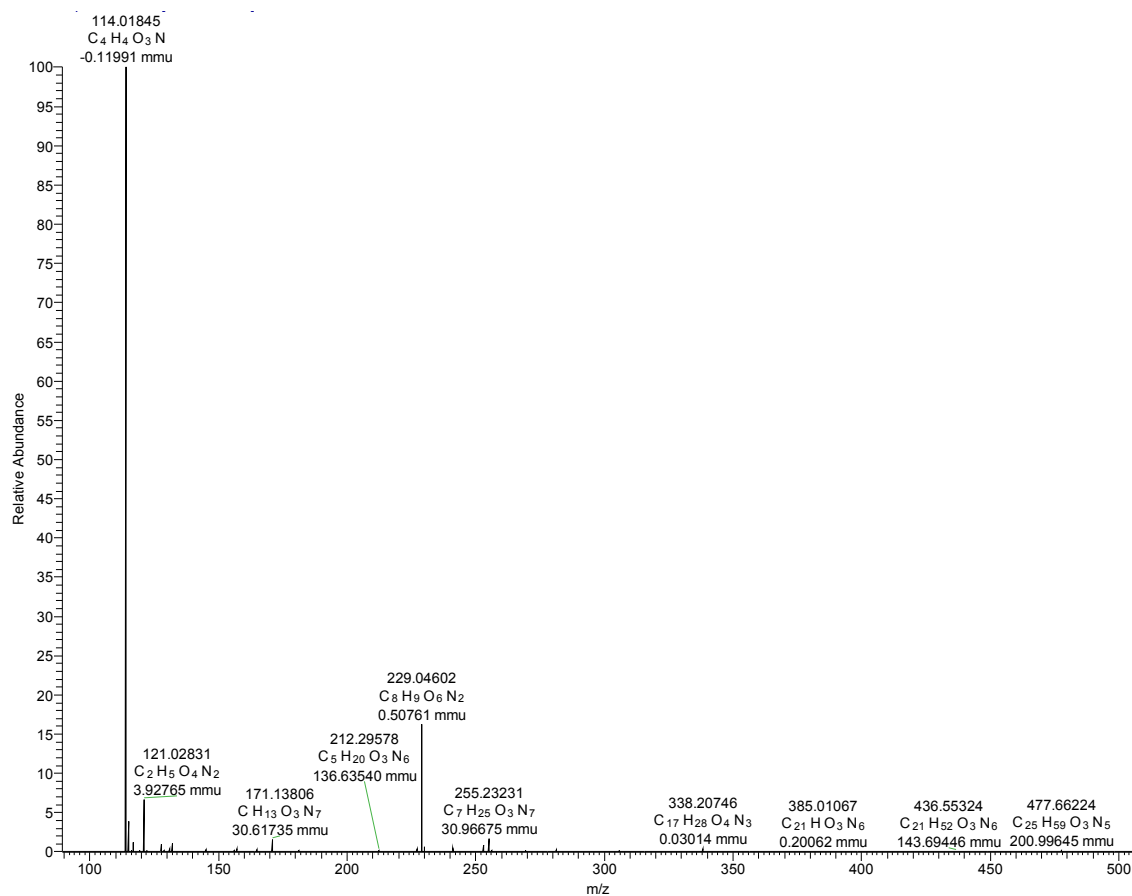


Figure S4. Negative mode DART-Orbitrap mass spectrum from m/z 90-500 of **S3**. Peak at m/z 114.01845 is $[M-H]^-$ and peak at m/z 229.04602 is $[2M-H]^-$, where M is 3 (N-hydroxysuccinimide, NHS).

c) Mass spectrum of **S4**

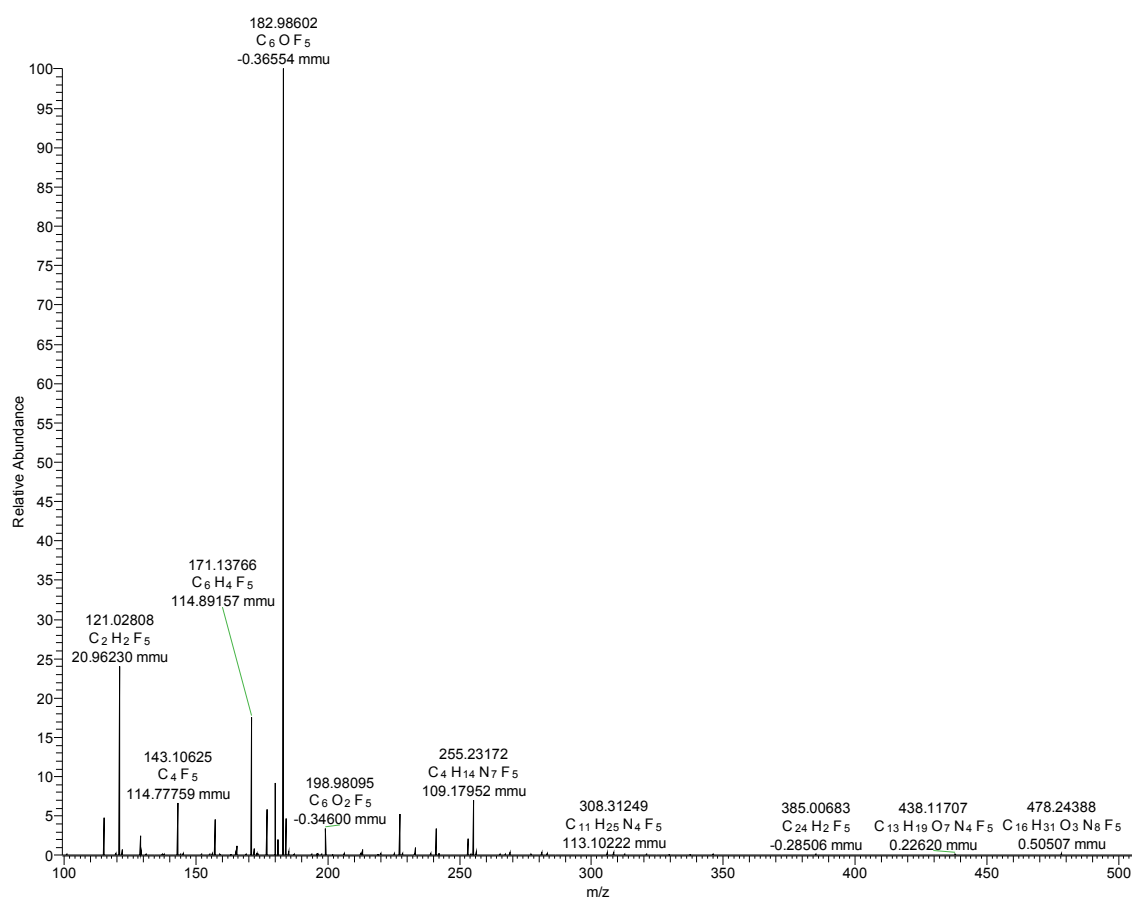


Figure S5. Negative mode DART-Orbitrap mass spectrum from m/z 100-500 of **S4**. Peak at m/z 182.98602 is $[M-H]^-$, where M is 4 (pentafluorophenol, PFP).

d) Mass spectrum of **S5**

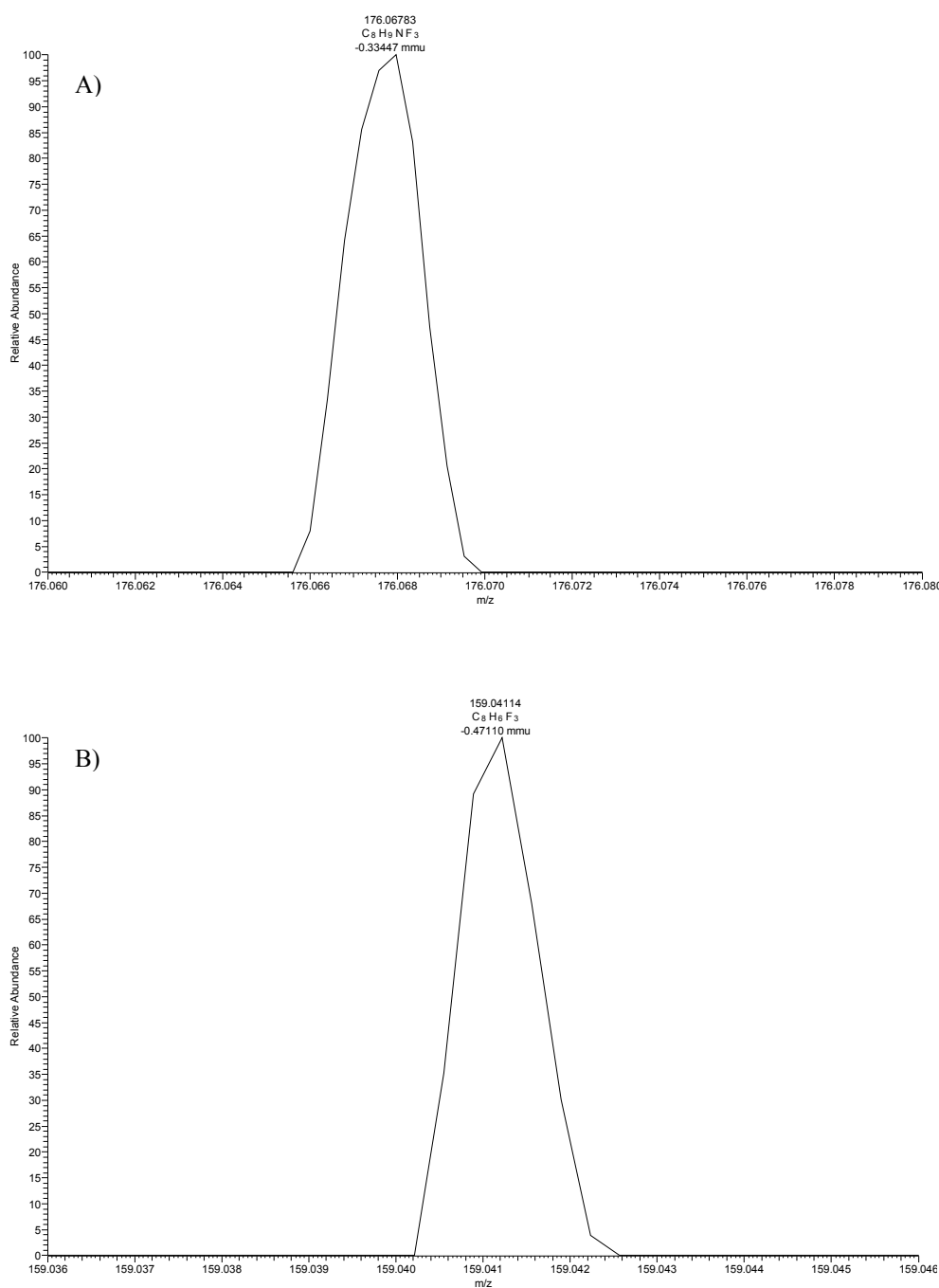


Figure S6. Positive mode DART-Orbitrap mass spectrum of **S5**; a) from m/z 176.06–176.08; peak at m/z 176.06783 is $[M+H]^+$, where M is **5** (4-(trifluoromethyl)benzylamine). b) from m/z 159.036–159.046; peak at m/z 159.04114 is $[M+H-NH_3]^+$, where M is **5** (4-(trifluoromethyl)benzylamine).

e) Mass spectrum of **S6**

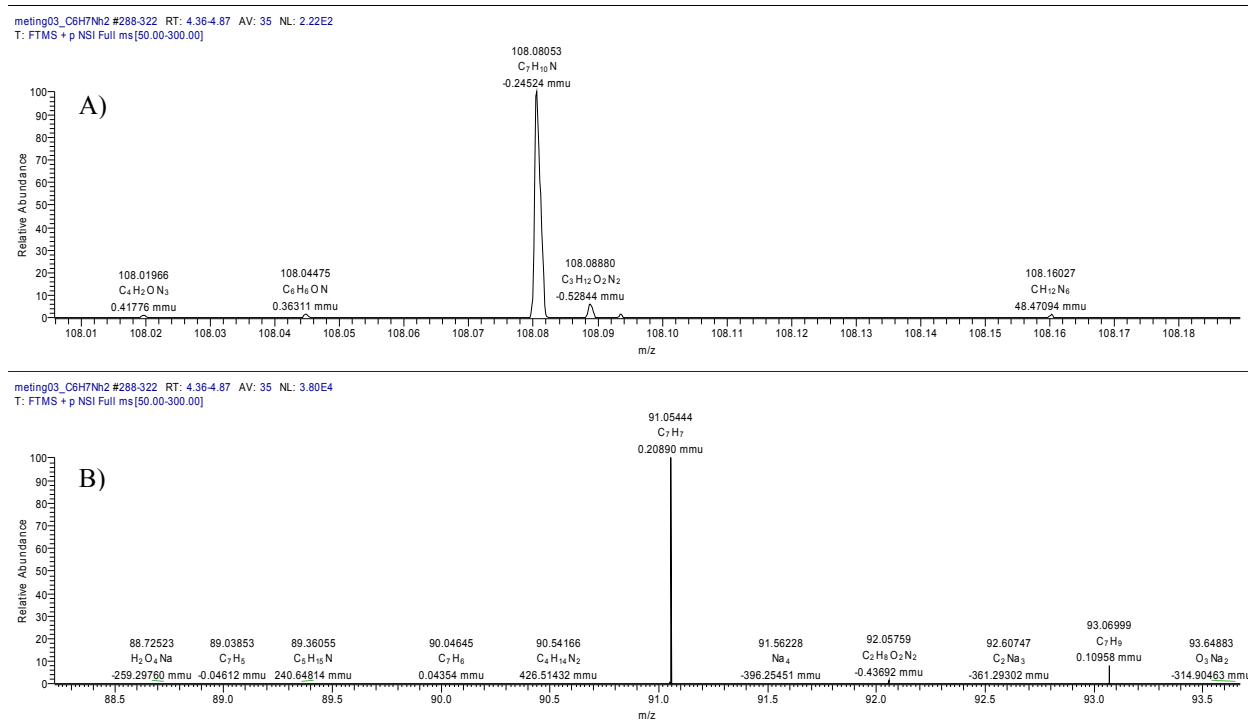


Figure S7. Positive mode DART-Orbitrap mass spectrum of **S6**: a) from (m/z 108.0-108.19); peak at m/z 108.08053 is $[\text{M}+\text{H}]^+$, b) from m/z 88.2-93.6; peak at m/z 91.0544 is $[\text{M}+\text{H}-\text{NH}_3]^+$, where M is **6** (benzylamine).

f) Mass spectrum of **S10**

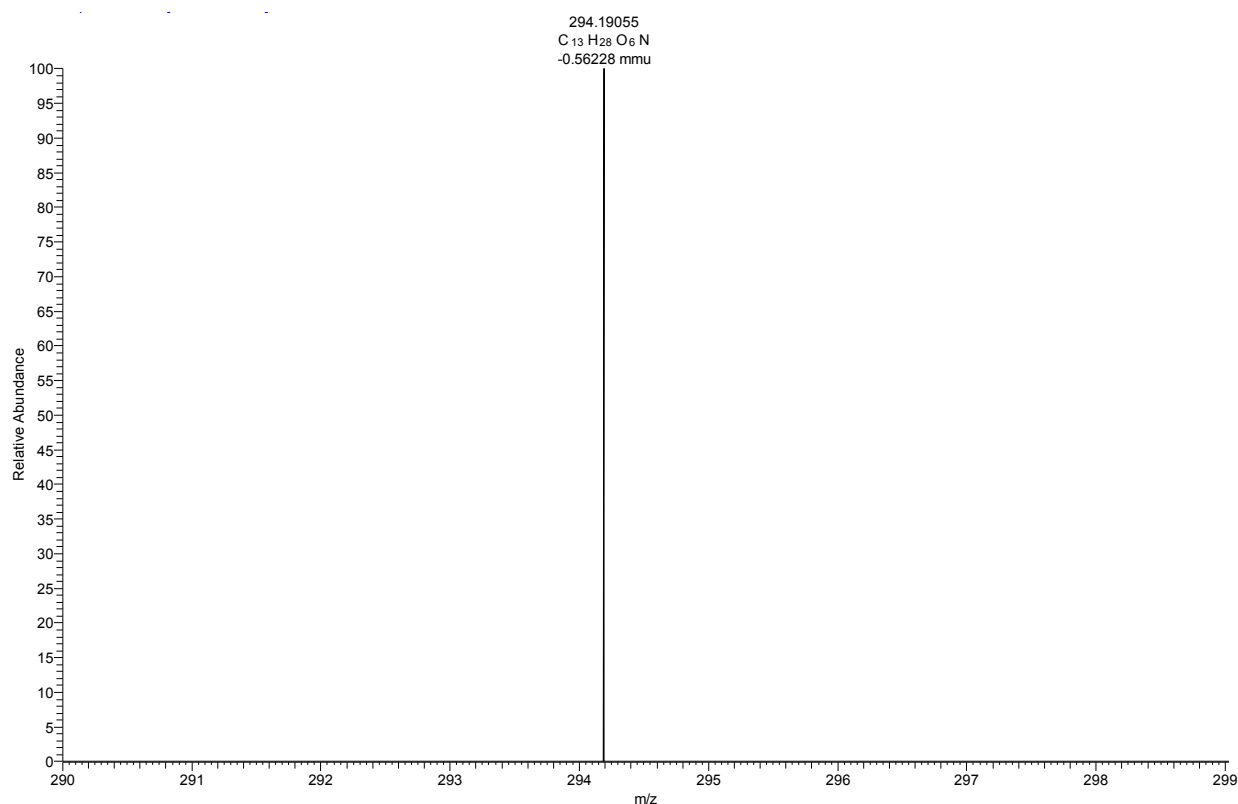


Figure S8. Positive mode DART-Orbitrap mass spectrum of **S10** from (m/z 290.0-299.0); peak at m/z 294.19055 is $[M+H]^+$, where M is **10** (2-aminomethyl-18-crown-6).

g) Mass spectrum of **S11**

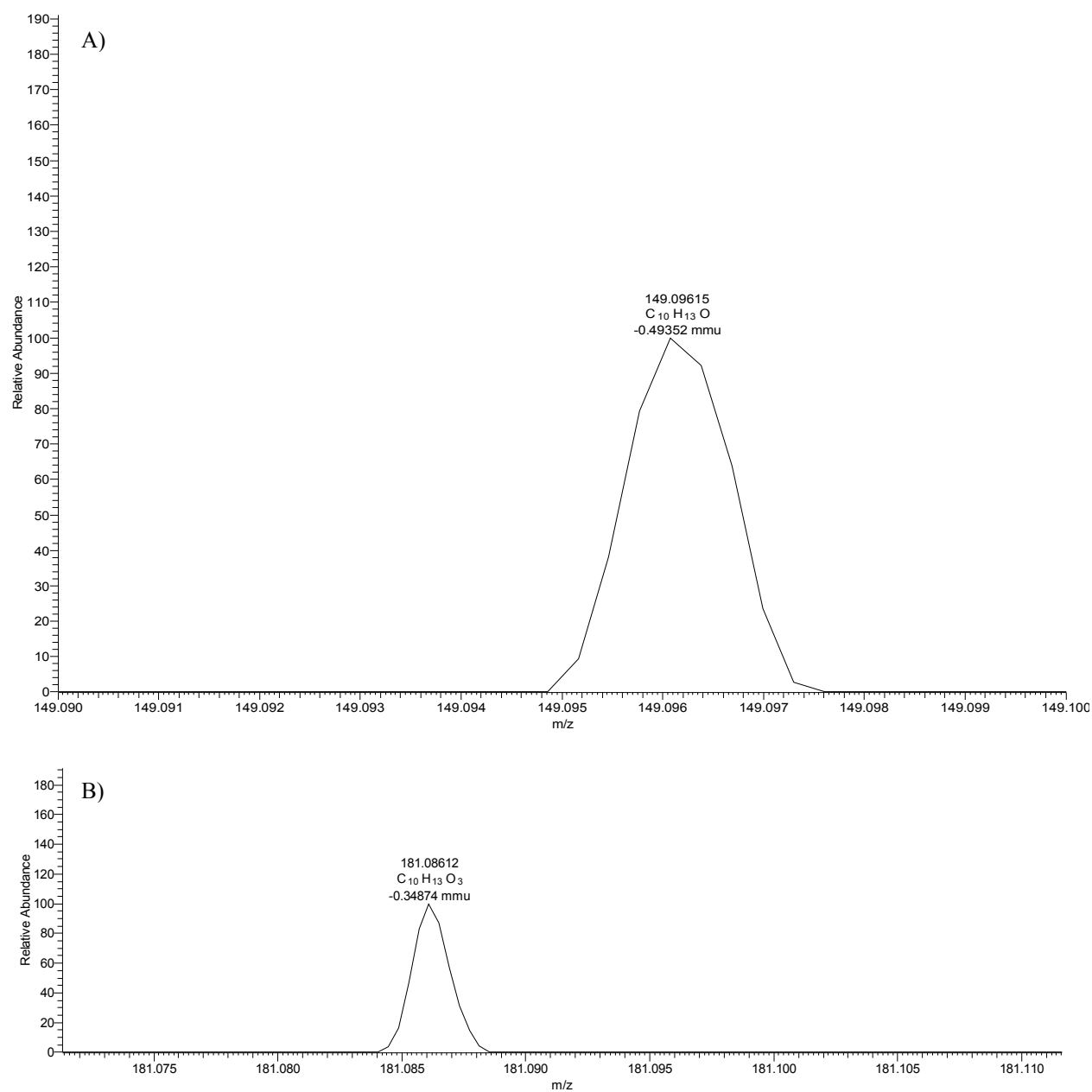


Figure S9. Negative mode DART-Orbitrap mass spectrum of **S11**, a) from m/z 149.09–149.10; peak at m/z 149.09615 is $[M-H]^-$. b) m/z 181.07–181.11; peak at m/z 181.08612 is $[M+20-3H]^-$, where M is **12** (¹R,⁸S,⁹s)-bicyclo[6.1.0]non-4-yn-9-ylmethanol).

h) Mass spectrum of \mathbf{S}_{mix}

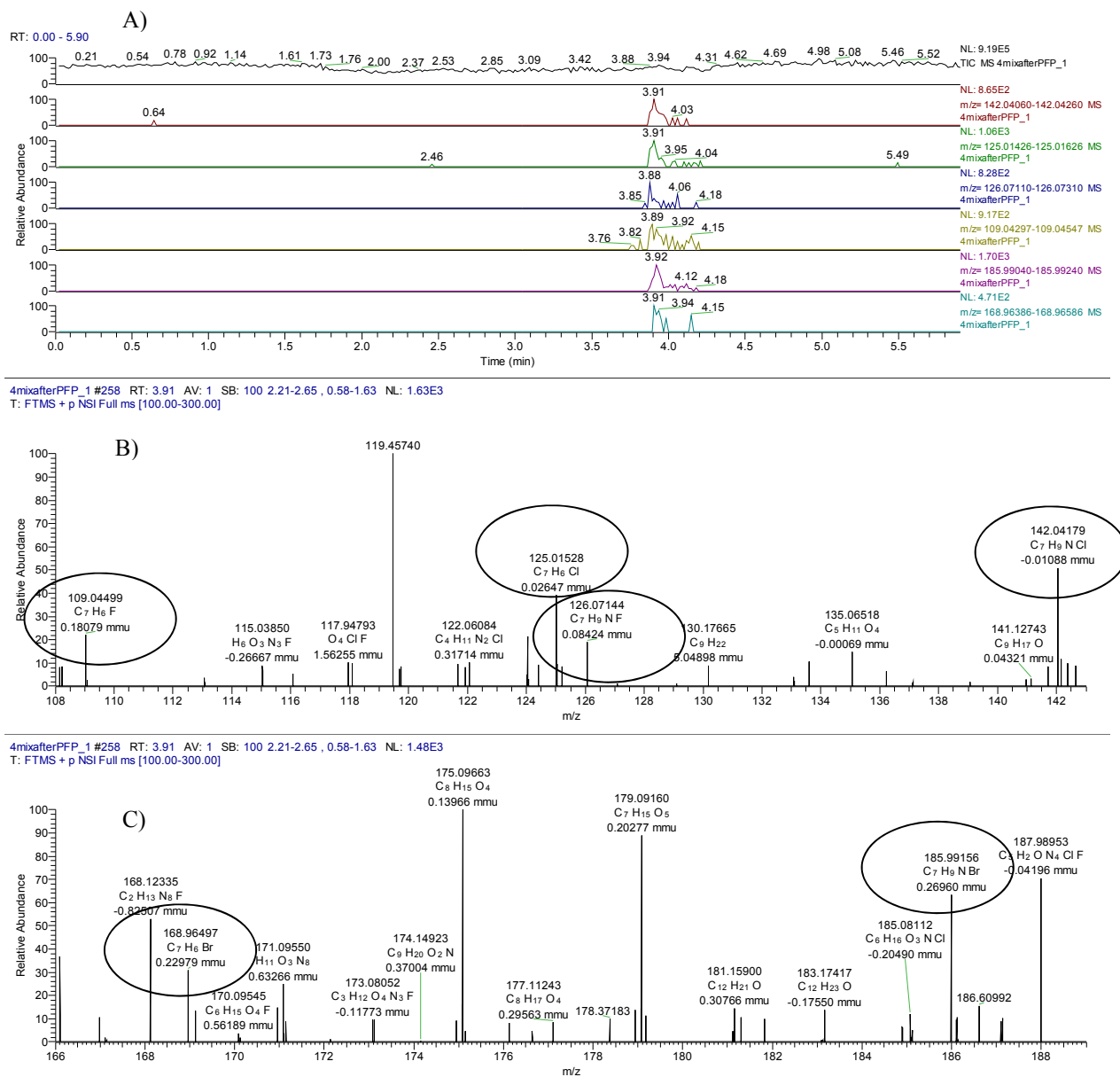


Figure S10. Positive mode DART-Orbitrap mass spectrum of \mathbf{S}_{mix} . A) Chronograms of mixed monolayer \mathbf{S}_{mix} . from top to bottom: TIC; EIC of m/z 142.0418 for $[\text{M}+\text{H}]^+$ of **8**; EIC of m/z 125.0153, for $[\text{M}+\text{H}-\text{NH}_3]^+$ of **8**; EIC of m/z 126.0714 for $[\text{M}+\text{H}]^+$ of **7**; EIC of m/z 109.0449 for $[\text{M}+\text{H}-\text{NH}_3]^+$ of **7**; EIC of m/z 185.9915 for $[\text{M}+\text{H}]^+$ of **9**; EIC of m/z 168.9649 for $[\text{M}+\text{H}-\text{NH}_3]^+$ of **9**. B) mass spectrum of \mathbf{S}_{mix} from m/z 108.0-143.0. from left to the right: m/z 109.0449 for $[\text{M}+\text{H}-\text{NH}_3]^+$ of **7**; m/z 125.0153 for $[\text{M}+\text{H}-\text{NH}_3]^+$ of **8**; m/z 126.0714 for $[\text{M}+\text{H}]^+$ of **7**; and of m/z 142.0418 for $[\text{M}+\text{H}]^+$ of **8**. C) mass spectrum of \mathbf{S}_{mix} from m/z 166.0-188.0. from left to the right: m/z 168.9650 for $[\text{M}+\text{H}-\text{NH}_3]^+$ of **9** and m/z 185.9916 for $[\text{M}+\text{H}]^+$ of **9**.

3. XPS analysis of monolayers **S1-S6, S10, S11, S_{mix}**

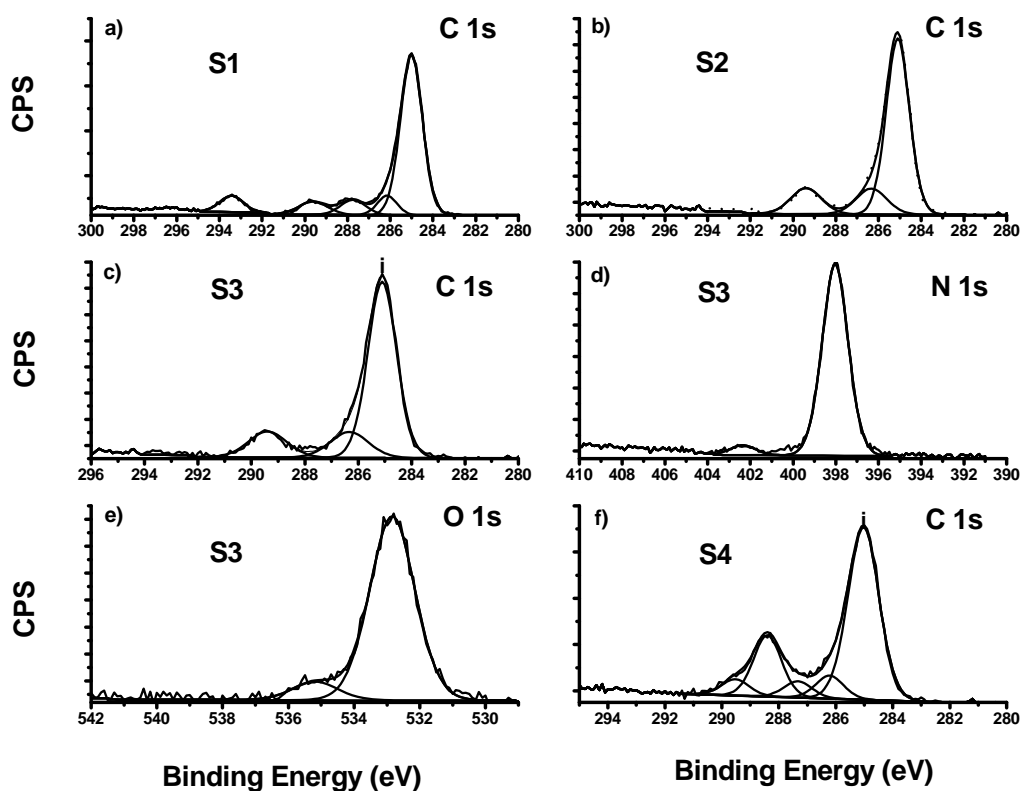


Figure S11. XPS high resolution C 1s spectra for a) **S1**; b) **S2**; c) **S3**; f) **S4**; and d), e) XPS high resolution spectra of N1s and O1s for **S3**.

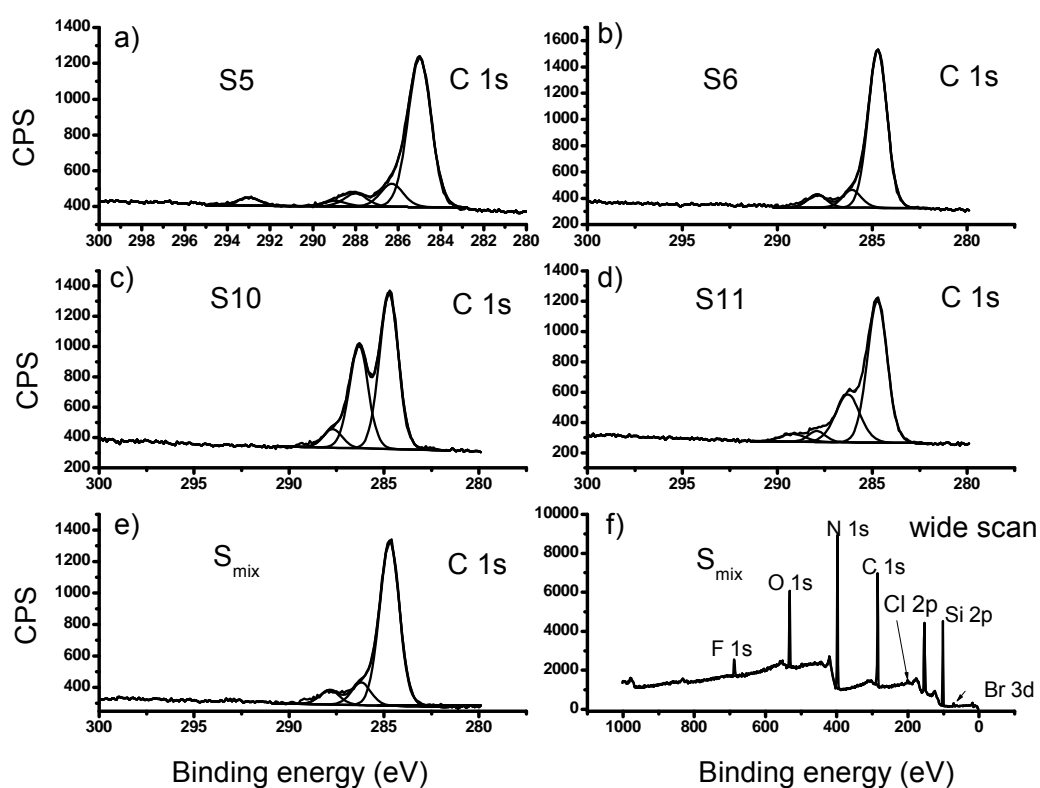


Figure S12. XPS high resolution C 1s spectra for a) S5; b) S6; c) S10; d) S11; and e) S_{mix}. f) XPS wide scan of S_{mix}.

4. Detected ions on monolayers **S1-S11** and **S_{mix}**

Table S1. Detected ions on monolayers **S1-S11** and **S_{mix}**

Compound	Selected fragments	Mono-layer ^[a]	Observed m/z on surface ^[b]	Calculated m/z ^[c]
1 C ₁₃ H ₂₁ F ₃ O ₂	[M+H] ⁺	n.d.	n.d. ^[a]	267.1566
	[C ₂ H ₃ OF ₃ -H] ⁻ [CF ₃] ⁻	S1	99.0054 68.9949	99.0058 68.9946
2 C ₁₁ H ₂₀ O ₂	[M-H] ⁻	n.d.	n.d.	183.1385
3 C ₄ H ₅ NO ₃	[M-H] ⁻ [2M-H] ⁻	S3; S5 S3	114.0184 229.0460	114.0185 229.0455
4 C ₆ HF ₅ O	[M-H] ⁻	S4	182.9860	182.9863
5 C ₈ H ₈ F ₃ N	[M+H] ⁺	S5	176.0678	176.0681
	[M+H-NH ₃] ⁺	S5	159.0414	159.0416
	[M+O-3H] ⁻	S5	188.0307	188.0317
	[M+2O-NH ₃ -3H] ⁻	S5	189.0150	189.0157
	[C ₈ H ₄ F ₃ O ₂ -CO] ⁻	S5	161.0212	161.0208
	[C ₇ ¹³ C ₁ H ₄ F ₃ O ₂] ⁻	S5	190.0180	190.0191
6 C ₇ H ₉ N	[M+H] ⁺	S6	108.0805	108.0802
	[M+H-NH ₃] ⁺	S6	91.0544	91.0542
10 C ₁₃ H ₂₈ N O ₆	[M+H] ⁺	S10	294.1906	294.1911
12 C ₁₀ H ₁₄ O	[M-H] ⁻	S11	149.0961	149.0960
	[M+2O-H] ⁻	S11	181.0861	181.0859
7 C ₇ H ₈ FN	[M+H] ⁺	S_{mix}; S7	126.0714	126.0714
	[M+HNH ₃] ⁺	S_{mix}; S7	109.0449	109.0448
8 C ₇ H ₈ CIN	[M+H] ⁺	S_{mix}; S8	142.0418	142.0418
	[M+H-NH ₃] ⁺	S_{mix}; S8	125.0153	125.0153
9 C ₇ H ₈ BrN	[M+H] ⁺	S_{mix}; S9	185.9915	185.9913
	[M+H-NH ₃] ⁺	S_{mix}; S9	168.9649	168.9647

[a] n.d. – not detected;

[b] for description of **S1-S11** and **S_{mix}** see scheme 1;

[c] calculated with XCALIBUR software (v. 2.1)

5. Limit of detection of DART-HRMS

As the reaction of pure amine with **S4** proceeded with 67% yield (**S1** = 100%; surface density for **S1** $\sim 4 \times 10^{14}$ molecules/cm²),^[1] the reaction with a mixture of three amines, having similar reactivity, should lead to a $\sim 22\%$ final surface density for each amide. Thus, for **S_{mix}**, the density of **7**, **8** or **9** separately would be $\sim 9 \times 10^{13}$ molecules/cm². As the absolute intensity of each ion was ~ 20 times higher than the lowest detectable signal (~ 50), the limit of detection of DART-HRMS is $\sim 5 \times 10^{12}$ molecules/cm², i.e. in the pmol range.

6. References

- [1] R. K. Manova, S. P. Pujari, C. A. G. M. Weijers, H. Zuilhof, T. A. van Beek, *Langmuir* **2012**, *28*, 8651-8663.
- [2] A. Kaufmann, S. Walker, *Rapid Commun. Mass Spectrom.* **2012**, *26*, 1081-1090.

7. Acknowledgements

This work is co-financed by the INTERREG IV A Germany-Netherlands program through EU funding from the European Regional Development Fund, the MWEBWV Ministry of North-Rhine Westphalia, the Dutch Ministry of Economic Affairs, Province of Gelderland, and the program management Euregio Rhein-Waal.